JOURNAL OF APPLIED ELECTROCHEMISTRY 25 (1995) 707–715

Effects of electrochemically incorporated bismuth on the discharge and recharge of electrodeposited manganese dioxide films in 9 M aqueous KOH

C. G. CASTLEDINE, B. E. CONWAY

Chemistry Department, University of Ottawa, Ottawa, K1N 6N5, Canada

Received 1 June 1994; revised 13 January 1995

Previous reported work has demonstrated that MnO_2 can be made multiple rechargeable over the two-electron capacity by chemical modification through incorporation of a small concentration of Bi(III) species. In the present work, conditions required for inclusion of bismuth species in electrolytically produced MnO_2 deposits on porous graphite are reported together with resulting electrochemical effects of the bismuth species on rechargeability of the electrodeposited MnO_2. The optimum conditions for deposition were found to be: temperature 85–90 °C; bath composition 0.5 to 2 M H_2SO_4, 0.5 M $MnSO_4$, 0.005 to 0.01 M Bi^{3+} and current density 5 to 20 mA cm^{-2} (apparent). The mechanism proposed for the inclusion of bismuth species is by continuous precipitation caused by high local acidity generated at the electrode by the reaction of anodic deposition of MnO_2. With respect to the mechanism of reduction and reoxidation of MnO_2 in 9 M KOH with bismuth species present, a previously suggested role of soluble intermediates is confirmed. It is proposed that bismuth may aid in the nucleation and growth process associated with formation of $Mn(OH)_2$ or MnO_2 from a soluble Mn(III) intermediate. Such a process must take place in order for completion of either discharge or recharge to take place at the electrode. It seems that the role of the included Bi species is to promote a discharge and recharge mechanism of the so-called 'heterogeneous' kind involving a soluble Mn(III) intermediate over an alternative, solid-state, 'homogeneous' pathway.

1. Introduction

Induction of multiple rechargeability in MnO_2 battery cathode material by chemical modification, using small mole fractions of Bi(III) or Pb(II) species, has been demonstrated by Wroblowa *et al.* [1–6]. This discovery is of major fundamental and potential practical significance. It is the purpose of the present work to examine if similar rechargeability of anodically prepared compact 'electrolytic MnO_2' films can be induced by codeposition of Bi species. First, we review attemps to establish rechargeability of bulk MnO_2.

Considerable efforts have already been made in attempts to achieve rechargeability of alkaline MnO_2 batteries. There are currently two directions of work on this subject: Kordesch and coworkers [7] have developed cells in which the depth of discharge of regular γ-MnO_2 cathode material is strictly limited (<35% of one electron capacity) while Wroblowa *et al.* [1, 6] and, more recently, our own research group have concentrated on investigations on MnO_2 doped with foreign metal ions such as Bi^{3+} or Pb^{2+}, or corresponding oxides. The original work in the latter area was initiated at Ford Scientific Laboratory, as described in publications [1–4] and patents [5, 6] issued since 1984.

The mechanism of discharge of γ-MnO_2 has been the subject of many investigations [8–19]. While there is not full consensus on the mechanism of the second-electron reduction stage, there is general agreement that the first-electron reduction involves a so-called homogeneous reaction involving 'proton insertion' coupled with electron transfer as proposed by Kozawa and Powers [9]: $MnO_2 + H_2O + e^- \rightarrow Mn.O.OH + OH^-$. The term 'homogeneous' refers to a mechanism where no phase changes occur and the process is characterized by a continuously sloping discharge curve that is due [9] to a Nernst redox-type relationship [20, 21] for oxidized and reduced species together in an homogeneous phase: $E = E^0 + (RT/F)\ln\{[Mn^{4+}]_{solid}/[Mn^{3+}]_{solid}\}$.

For conditions where there is conversion of one solid phase to another, the potential during the discharge should remain virtually constant because the activities of the two solid phases do not depend on the quantity of active species present until one or the other is completely consumed, i.e., $E = E^0 + RT/F \ln a_{ox}/a_{red}$, where a_{red} and a_{ox} are, for this case, constant throughout the discharge for the nominally pure, coexistent phases.

Kordesch *et al.* [7] have shown that there is a logarithmic relationship between the depth of discharge and the number of discharge–recharge cycles that can be realized with depths of discharge up to 60% of the *one-electron* capacity of γ-MnO_2, being restricted by anode (Zn) limitation. In contrast, the

0021-891X

work of Wroblowa *et al.* [2–6] and subsequent research in our laboratory [22] indicates that the so-called chemically modified (CM) MnO_2 is not γ-MnO_2 and behaves in a remarkably different way from it under discharge and recharge.

Chemically modified material is produced by rendering basic a solution of Mn^{2+} and Bi^{3+} (or Pb^{2+}), then oxidizing the precipitated mixture by bubbling with oxygen. Bismuth, thus incorporated, has a substantial effect on rechargeability when present in as little as 2 mol % [4] but it is usually added in the range of 7 to 12 mol %. It does not itself contribute to the charge capacity of the MnO_2 as the reduction potential lies below the point where completion of reduction of MnO_2 occurs.

With the chemically modified material, little deterioration in discharge behaviour is observed even after hundreds of cycles to 80% of the 'two electron' capacity and the recent work shows that the reaction then takes place substantially via an heterogeneous pathway through some fraction of the charge for the first and over most of the second electron reduction stages and corresponding re-oxidations [22]. Detailed work on the redox mechanisms of the CM MnO_2 system has been the subject of the research of others in this group (cf. [22]) and is not the main topic of the present paper.

In the present research we have produced bismuth-containing MnO_2 by directly codepositing bismuth (III) species with MnO_2 electrolytically generated on porous graphite rods according to well known procedures [8, 23–25]. The observation and characterization of the rechargeability of the resulting deposited material is the main aim of the present work.

2. Experimental details

2.1. *Deposition experiments*

All electrochemical depositions of MnO_2 were carried out at 85 °C in a thermostated cell as in [8]. The counter and working electrodes were made from graphite rods (Johnson Matthey Electronics, Ward Hill, MA) of 99.999% purity which were machined to the required length (5 or 1 cm length exposed after mounting in a Teflon holder with the ends being faced on a lathe). A saturated calomel electrode (SCE) was used as the reference electrode to control the electrode potentials at which the depositions were carried out.

In the deposition experiments, anodic electrolyses were conducted under galvanostatic control at 85 °C for a fixed period of time, so that the total coulombs passed could be determined and hence the amount of material which should ideally be deposited could be calculated. After the deposition, the MnO_2 coated electrodes were removed from the bath and from their holders, then soaked in distilled water for at least overnight before use in further experimentation. Samples that were sent for SEM/EDX analysis, were dried in a vacuum oven at about 65 °C for 1 h. No further preparation was necessary.

Although a variety of deposition bath compositions, employing various anodic and cathodic current densities were tried, the basic deposition experiment was always done in the same way. New graphite working electrodes were first soaked briefly in sulphuric acid then in distilled water until used. For electrical connection, a copper wire was secured to the electrode using a brass screw and nut.

For the MnO_2 deposition bath, $MnSO_4$ was dissolved in 0.5 M sulphuric acid solution [23–25]. Other acidic baths in which nitric, perchloric and hydrochloric acids were substituted for sulphuric acid, were tried in an attempt to increase the extent of codeposition of bismuth in the deposits. However, these other acids did not provide good smooth and adherent deposits of manganese dioxide and AAS results for the Mn/Bi ratios were erratic. The chemicals used for all experiments were of analytical or higher grade and were not subjected to further purification.

Bismuth metal has a limited solubility in sulphuric acid and no commercially available bismuth sulphate was found. Bismuth metal was therefore heated vigorously with a small amount of sulphuric acid to dryness. The required amount of acid for the deposition bath was then added carefully to the white residue and heated again before being diluted to the required volume (typically 200 cm^3 in the 250 ml vessel used as the deposition cell).

2.2. *Instrumentation and methods*

A Hokuto Denko HA-501 potentiostat/galvanostat (Tokyo, Japan) was used as a power source for all of the deposition experiments. SEM and EDX facilities (Nanolab 7 and a Kevex EDX detector) were used for photomicrography and near-surface analyses.

Atomic absorption measurements were performed using a Varian Techtron AA-1475 instrument (Mulgrave, Australia). Determinations were made on the MnO_2 + Bi oxide materials using manganese standards produced from Mn metal (Alfa-Ventron, Danvers, MA) by an appropriate dissolution procedure. Bismuth standards for AAA were prepared from 99.99% Bi_2O_3 (Aldrich Chemical, Milwaukee, WI) by dissolution and subsequent dilution in 5% v/v/aq. HCl. Solution samples for AAS analysis were simply diluted in 5% v/v/aq. HCl. MnO_2 deposits for analysis were first dissolved in the appropriate amount of aq. HCl to give a final concentration of 5% v/v.

2.3. *Cyclic voltammetry experiments*

For cyclic voltammetry experiments, an Hokuto Denko HA-501 potentiostat/galvanostat was employed in conjunction with an HB-104 function generator from the same manufacturer. Data were

collected digitally on a Nicolet 2090 digital oscilloscope (Madison, WI) and transferred to an HP 9000 series 216 computer via an IEEE interface. The data were processed and plotted on an HP 7470A plotter using Basic software developed in this laboratory.

During the cyclic voltammetry experiments on MnO_2 deposited on porous graphite, UHP grade, oxygen-free nitrogen gas was used for purging the electrochemical cell.

2.4. *Cells*

Two electrochemical cells of the standard three-compartment design were used and the electrolyte was 9 M KOH. The electrode arrangement in the larger cell, constructed of Teflon, is shown in Fig. 1. The reference electrode used for all experiments was Hg/HgO in aq. 9 M KOH and was constructed of glass in the usual way.

The other electrochemical cell, referred to as the 'rod end' cell, shown in cross section in Fig. 2, was designed to conduct experiments on the flat end of a test electrode in a small volume (1 or 2 drops) of electrolyte. The working electrode was lowered into the compartment until it contacted the separator material, and the only electrolyte remaining was that which was not squeezed out during this procedure. The reference electrode capillary was dipped into the 'reference electrode compartment' and a nickel mesh as counter electrode was mounted in the compartment containing that electrode.

For experiments in the 'large' cell, the apparatus was purged with nitrogen for at least 1 h before beginning the experiment. Cyclic voltammetry experiments were usually conducted at sweep rates of 5 or $10\,mV\,s^{-1}$ as noted elsewhere in the text, initially in the cathodic direction, since the deposits were in the 'charged' MnO_2 state.

3. Results and discussion

3.1. *Properties of deposits of MnO_2*

The optimal conditions for deposition of bismuth-containing MnO_2 deposits, as found in this study, were as follows: temperature 85–90 °C; bath composition 0.5 to 2 M H_2SO_4, 0.5 M $MnSO_4$ and 0.005 to 0.01 M Bi^{3+}; current density 5 to $20\,mA\,cm^{-2}$ (apparent).

The colours of the deposits from 0.5 M H_2SO_4 ranged from grey to black when current–densities of 5 to $20\,mA\,cm^{-2}$ were used. They also had a relatively rough appearance for short deposition times but were usually smooth for longer depositions. All deposits were adherent and the inclusion of bismuth had no apparent effect on the morphology of the deposit.

The results of two sets of typical atomic absorption analyses are presented in Table 1. Note that in the first experiment, one electrode was simply soaked in the deposition bath without passage of current. This 'blank' experiment showed that the inclusion of bismuth from sulphuric acid baths is not simply from absorbed electrolyte. Both experiments show that the Mn/Bi ratio is about the same for depositions of different durations at the same current density; in one case, 5 for 50 min and in the other, 10 for 30 min. Therefore, the bismuth was being included into the deposit on a continuous basis. It is unusual that bismuth should be deposited from solution at the potentials used for electrodeposition of MnO_2 as this potential lies well above the reversible potential for the Bi^{3+}/Bi^0 couple (0.317 V vs SHE [BiO^+/Bi]) [34] but well below the potential for the Bi^{5+}/Bi^{3+} couple (2.0 ± 0.2 V vs SHE [34]).

Figure 3 shows SEM micrographs of the face of a graphite rod, with and without electrodeposited MnO_2. The initial graphite surface is quite rough in appearance, showing many cracks and pores. The black deposited surface which has a macroscopically smooth morphology, shows a dried 'mud pack' like appearance under magnification probably caused by contraction of the deposit when it is dried. SEM cross-section micrographs of these deposits showed a thickness consistent with the bulk density of MnO_2 and the faradaic charge passed to make the deposit.

To investigate further the mode of inclusion of bismuth in the MnO_2 deposits, attempts were made to form bismuth deposits anodically in a bath containing 0.005 M Bi(III) in 0.5 M H_2SO_4 with no manganese present. Under galvanostatic conditions at $+11\,mA\,cm^{-2}$, the expected reaction at the working electrode would be the evolution of oxygen. During the 10 min of passage of current, the working electrode–reference electrode potential difference dropped slowly from 1.59 to 1.46 V vs SCE, gas evolution being continuously observed. When inspected by SEM, the electrode thus produced was seen to have clusters of crystals grown upon it in Fig. 4, with ca. 40 observable per mm^2. EDX analysis of the cluster portrayed in Fig. 4 indicated a high bismuth content and evidence of sulphur consistent with the crystals being a sulphate of bismuth; thus 'bismuth' is depositable, by itself, under the above conditions.

Because the working-reference electrode potential difference in the above experiment was close to the potential at which Bi^{3+} could become oxidized to Bi^{5+}, the procedure was repeated under potentiostatic conditions at 1.4 V vs SCE, i.e., below the potential for oxidation of Bi^{3+}. Current was passed for 20 min and ranged from 12 mA at the beginning to 35 mA at the end of the experiment. This time, the scanning electron micrograph did not show clusters and, in fact, the electrode surface looked clean. However, EDX analysis showed that there was still some deposit of bismuth species on it.

3.2. *Solubility and speciation of Bi and Mn in deposition and in MnO_2 discharge and recharge*

The solubility of both bismuth and manganese was measured analytically over a large range of H_2SO_4

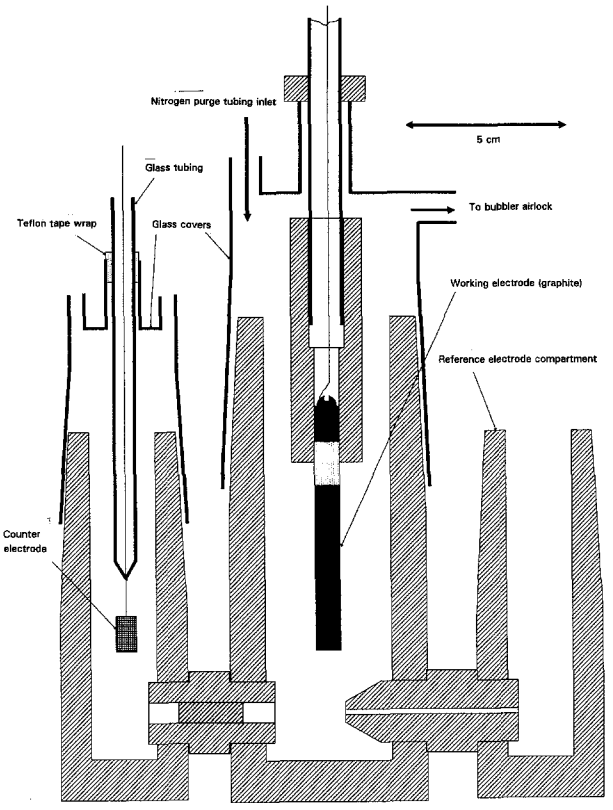

Fig. 1. Schematic diagram of 'large' cell used for electrochemical experiments.

concentrations both at room temperature and at 85 °C, the temperature typically used for MnO_2 deposition. The results are summarised in Table 2. These data confirm the fact that bismuth species are less soluble at higher temperatures than low, in moderately strong sulphuric acid. The other interesting point is that the solubility reaches a peak and declines somewhere in the range 1.5 to 15 M H_2SO_4. At 15 M, the solubility is greater at higher temperature. This indicates that the bismuth species, both solid and/or soluble, are not the same in highly concentrated H_2SO_4 as in solutions of moderate acid strength.

During the anodic deposition, the overall reaction at the electrode produces protons so that a buildup of protons occurs at/near the surface leading to a diminished local pH, dependent on anodic current density:

$$Mn^{2+} + 2H_2O \longrightarrow MnO_2 + 4H^+ + 2e^-$$

Charge neutrality is maintained by diffusion and electrolytic migration of anions. It is this drop in pH which is presumed to cause the chemical precipitation of bismuth species into the growing MnO_2 deposit. Note also that the coevolution of oxygen also produces protons and the deposition of bismuth species onto a bare graphite rod can be explained using the same arguments that are presented here.

The species of bismuth sulphate that is precipitated from a sulphuric acid solution is of interest here. Exploration of the classical inorganic chemistry literature, for example, the early work of Allan [26] and more recently that of Skramovsky and Vodrasek [27], indicates that a basic BiO^+ is generated at low sulphuric acid concentration and changes to a supposed BiH^{4+} species in almost pure sulphuric acid, although the Bi-species is then probably complexed with HSO_4^- ions. In 0.5 M H_2SO_4 the expected solubility equilibrium is

$$2BiO^+ + HSO_4^- \longrightarrow (BiO)_2SO_4 + H^+$$

It would not be expected that this equilibrium would be affected greatly by increases in sulphuric acid strength as the HSO_4^- and H^+ concentrations would both increase, keeping the equilibrium in balance. However, in this acid concentration range, the following protonation equilibrium has also to be taken into account:

$$BiO^+ + H^+ \rightleftharpoons BiOH^{2+}$$

This would explain the increase in solubility of bismuth species with acid concentration at moderate sulphuric acid strengths, noting that the salt of the $BiOH^{2+}$ species is more soluble than the salt of the BiO^+ species. As indicated by Allan [26], at about 7 M H_2SO_4 the dominant species changes again to Bi^{3+} or possibly BiH^{4+}. If this is the case, it can be seen that in the region of 7 M H_2SO_4 a very insoluble bismuth species can be expected to form. Of course, when the above anodic reaction of Mn^{2+} to MnO_2 which produces protons at the electrode is occurring, the sulphate concentration would not be affected but the influence of acid strength on the protonation reaction might be expected to be important in determining formation of the insoluble bismuth species. It is hard to predict the exact influence on the local acid strength due to the protons produced at the electrode surface but it does not seem unreasonable that a strength of 14 M in H^+ might be attained locally. Of course, the process of concentration of protons is opposed by their diffusion away from the boundary layer.

In summary, the generation of protons by the process of deposition of MnO_2 can cause a local increase in the acid strength near the electrode which can cause the protonation reaction to occur with subsequent precipitation of bismuth species, most probably $Bi_2(SO_4)_3$ or $BiH(SO_4)_2$.

In another part of this work, the solubility of Bi^{3+} species in 9 M KOH was determined. After allowing nine days for saturation equilibrium to be established between Bi_2O_3 and aq. 9 M KOH, the concentration of bismuth was measured in the supernatant by means of AAS and found to be 65 mg dm^{-3} or 3×10^{-4} M. This value is in moderate agreement with the value of 5.02×10^{-4} M reported by Wroblowa [2]. As for Mn species, this solubility is to be regarded as significant. However, since the bismuth species are generally not by any means in large enough quantities to contribute significantly to the charge capacity (typically 7–12 mol % Bi was used in the studies by Wroblowa [1] and in our laboratory [22]), the solubility of bismuth is of interest more because it may determine whether the action of the bismuth

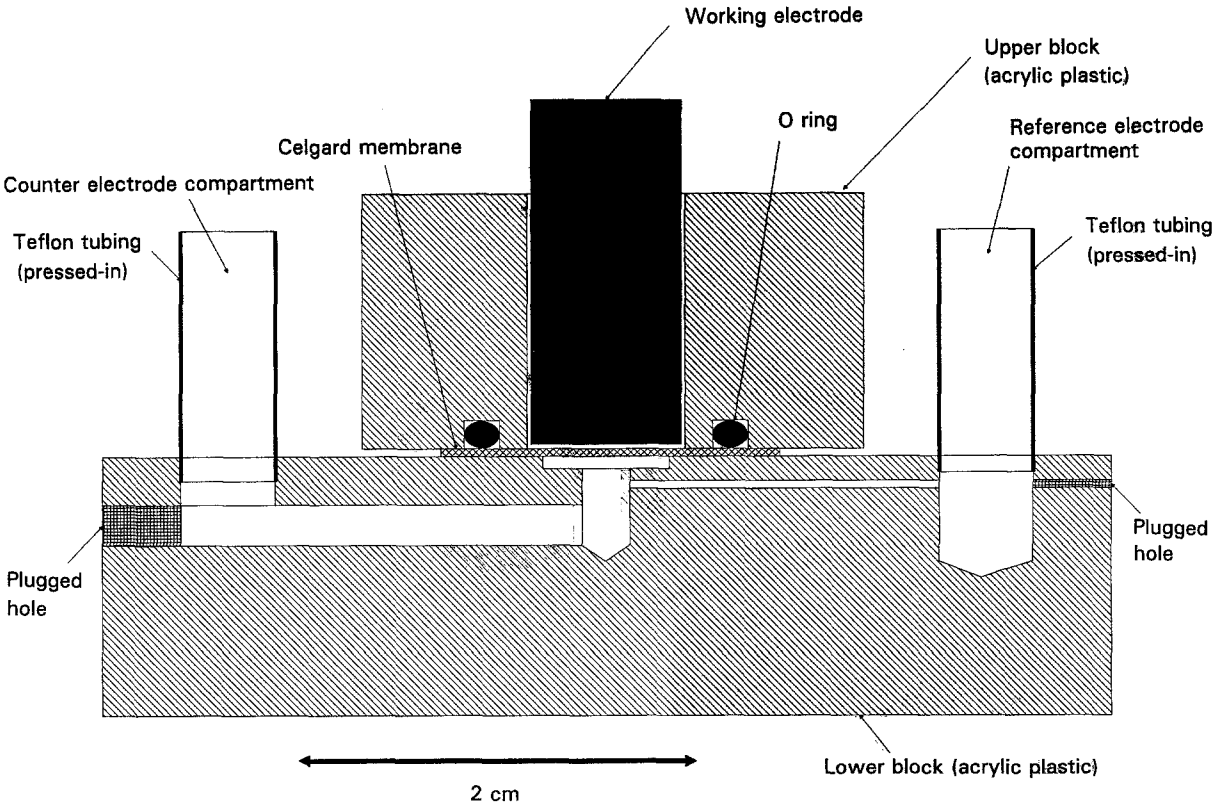

Fig. 2. Schematic diagram of 'rod-end' cell used for electrochemical experiments.

is related to solid–solid reactions, liquid–liquid reactions or solid–liquid reactions involving Mn species.

Solubility of manganese species is also an important factor [22, 28] in the study of the electrochemical discharge and recharge behaviour of the MnO_2 deposits in 9 M KOH and in operational aspects of the alkaline MnO_2 battery. Kozawa *et al.* [28] have determined the solubility of Mn^{2+} and Mn^{3+} species by a polarographic technique over a range of KOH and NaOH concentrations. In 9 M KOH, these were reported as 35 mg dm^{-3} (6.4×10^{-4} M) and 240 mg dm^{-3} (4.4×10^{-3} M), respectively. Lott and Symons [29] proposed that the Mn^{3+} exists as $Mn(OH)_6^{3-}$ in concentrated KOH solution. Spectroelectrochemical work in our own laboratory [22] indicates that soluble Mn^{3+} species play an important role in the overall mechanism of reduction of MnO_2, particularly when attempting to make a practical rechargeable MnO_2 battery and evaluate its performance. Thus, knowledge of the solubility of the various Mn and Bi species leads to at least one significant conclusion: that the design of any practical MnO_2 electrode system should provide for the absolute minimum of liquid electrolyte so that soluble intermediates and products will be unable to migrate away from or out of the electrode matrix and interfere with processes at the anode.

3.3. *Cyclic voltammetry experiments on MnO_2 deposits*

Electrochemical rechargeability of the deposits can be conveniently determined by means of cyclic voltammetry. Figure 5 shows the early cycling behaviour of MnO_2 deposited from 2 M H_2SO_4 with 0.5 M $MnSO_4$, conducted at a sweep-rate of 10 mV s^{-1} in

Table 1. Atomic absorption analyses of MnO_2 deposits

Bath composition	*Temp./* °C	*Galvanostatic conditions** /mA (apparent cm^2)$^{-1}$	*WE vs RE voltage* /vs SCE	*Manganese deposited* /μMol (apparent cm^2)$^{-1}$	*Coulombic efficiency*/%	*Bismuth deposited* /μMol (apparent cm^2)$^{-1}$	*Molar ratio Mn/Bi*
0.5 M Mn 0.005 M Bi	86	+10, 5 min	1.14	14	90	0.46	31
0.5 M H_2SO_4	85	soak 50 min (no current)	–	0.09	–	0.009	10
	86	+10, 50 min	1.16–1.40	127	82	3.5	36
0.5 M Mn 0.01 M Bi	85	+10, 10 min	1.18–1.26	27	87	1.2	23
2 M H_2SO_4	86	+10, 30 min	1.18–1.40	59	63	2.7	22

WE: working electrode. RE: reference electrode (SCE). * +ve indicates anodic current.

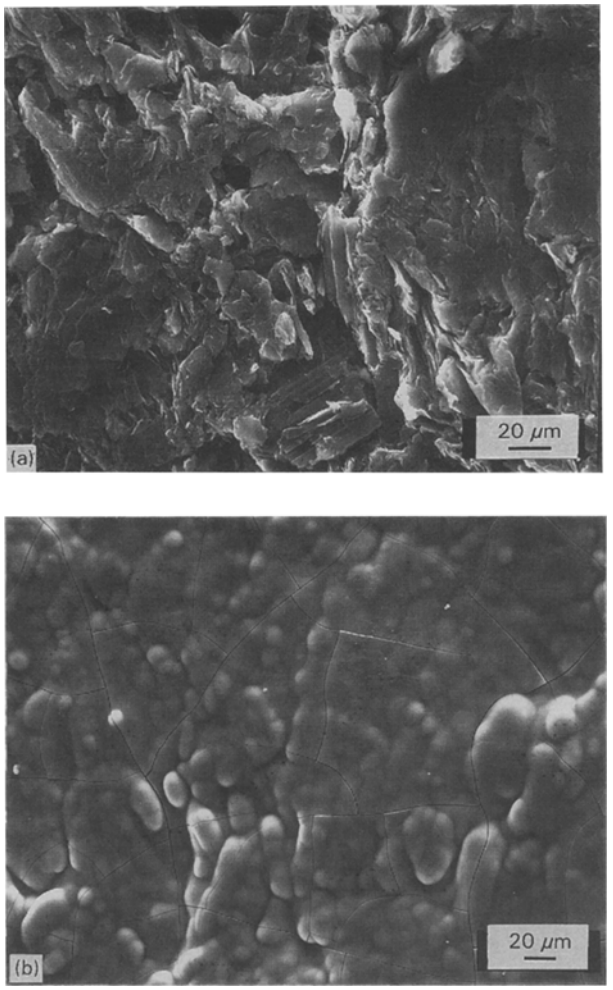

Fig. 3. SEM micrographs of the surface of a graphite rod: (a) without any deposit, (b) with deposited MnO_2 together with included bismuth species.

9 M aq. KOH. The upper (reference) voltammogram is for a deposit with *no* bismuth. The charge capacity, both anodic and cathodic, decreases continuously as the electrode is cycled. The lower voltammogram is for a deposit made in the same bath but saturated with Bi^{3+}. The initial concentration was 0.02 M but

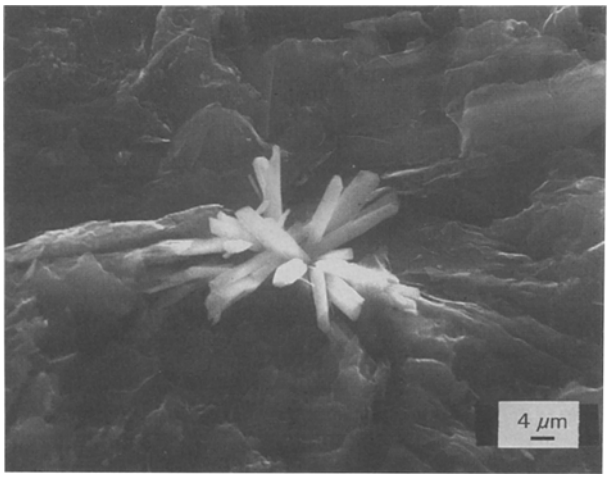

Fig. 4. SEM micrograph of a cluster of crystals of a bismuth compound on the surface of a graphite rod.

Table 2. Solubility of bismuth and manganese species in relation to sulphuric acid strength

H_2SO_4 concentration/M	Bismuth/mM		Manganese/M	
	Room temp.	*85 °C*	*Room temp.*	*85 °C*
0.05	1.2	0.3	>0.5	>0.5
0.15	2.1	1.1	>0.5	>0.5
0.5	8.9	5.9	>0.5	>0.5
1.5	16	11	>0.5	>0.5
5	>20	>20	>0.5	>0.5
15	<2.2	8.7	0.023	0.072

precipitation occurred as the bath was heated to 85 °C. However, based on the solubilities reported above, the concentration of bismuth should be between 0.01 and 0.02 M. The charge capacity for this deposit decreases for the first few cycles then increases back to about the original level and stays there for many cycles. Figure 6 shows the substantial longevity of the rechargeability of the deposit when bismuth is present in the material. The behaviour on the 40th and 640th cycles is shown.

Both deposits were made by passing 150 mC cm^{-2} with an efficiency that was typically ca. 90% corresponding to a realizable theoretical capacity of 135 mC cm^{-2}. Without bismuth, the cathodic capacity on the first cycle is 65% of this figure and soon becomes reduced to 25% or less after five cycles. For the deposit with bismuth, the cathodic capacity stays within the range 30 to 35% of the theoretical two-electron charge over the full 640 cycles of the test, or to within 88% of the initially realized experimental charge.

The anodic recharge capacities of the two deposits with respect to cycle number are summarized in Table 3. Note that the bismuth-containing deposit retains virtually all of its capacity during the 640 cycles whereas, without bismuth, the anodic capacity becomes reduced by 70% after only 30 cycles or less.

The charge for formation of a monolayer of MnO_2 may be calculated as 0.334 mC cm^{-2}, given a density of 4.85 g cm^{-3} [30] and a two-electron process. A roughness factor of 950 was determined for the graphite substrate used in these experiments by the BET method. This indicates that a charge of 317 mC cm^{-2} would be required for monolayer formation. While the BET area value is a good indicator of the effective surface area, not all of the surface may be electrochemically accessible [31, 32]. Notwithstanding this effect, it is apparent that what is seen in the cyclic voltammetry experiments is a reaction equivalent to less than a monolayer in extent.

In various series of cyclic voltammetry experiments, up to 640 cycles were achieved (Table 3). More can be attained in a starved electrolyte cell (cf. [22] and below) where loss of Mn(III) species into solution is minimized. In the first cathodic half-cycle on a new MnO_2 deposit without Bi, the cathodic charge is substantially larger than that on anodic recharge. Some of this apparent imbalance during the first cycle could be due to reduction of

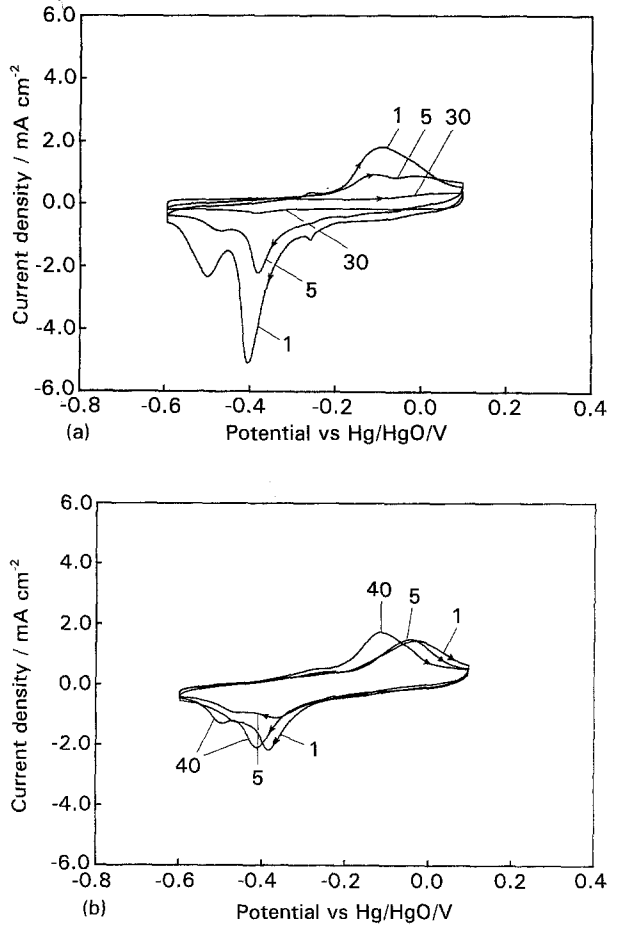

Fig. 5. The early cycling behaviour of deposits of MnO_2: (a) no bismuth present in the deposit, the 1st, 5th and 30th cycles are shown; (b) with bismuth species in the deposit, the 1st, 5th and 40th cycles are shown.

oxygen trapped or adsorbed in the deposit; however, most of the charge imbalance is due to loss of material during the cathodic half-cycle through dissolution of Mn(III) into the bulk electrolyte so that it is then unavailable for reoxidation in the subsequent anodic sweep. After a few cycles, this imbalance is much reduced but still persists. Using minimum free electrolyte, and for discharge/recharge beyond the first few cycles, up to 640 cycles (the maximum followed here) can be achieved (Fig. 6) with anodic/cathodic charge balances matching within about $5 \sim 7\%$ which is the limit of experimental error taking account of some changes of base-line in the voltammograms during long cycling. However, for MnO_2 deposits not containing bismuth, the ratio of cathodic to anodic recharge capacity is always somewhat higher than for the Bi-modified deposit, is one of the reasons for restricted rechargeability of MnO_2 without bismuth.

From the above, it is clear that not all of the deposit is available for undergoing electrochemical processes under these conditions. In fact, after cycling any of these deposits for an extended period, the electrolyte in a 'free electrolyte' cell becomes coloured and solid particles are found to be floating in the cell. This behaviour supports the existence of a soluble (Mn(III)) intermediate being formed in the charge–

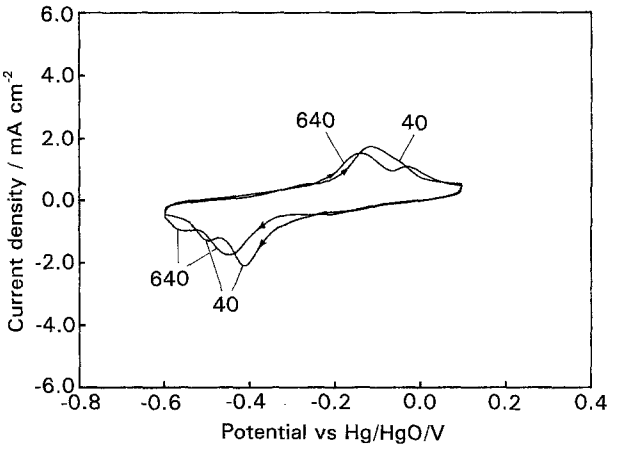

Fig. 6. Extended cycling of an MnO_2 deposit in 9 M aq. KOH with bismuth species included. The 40th and 640th cycles are shown.

discharge regime which can diffuse away from the electrode as is indeed observed in our own [22] and other work [8]. Also, Ruetschi [16] directly observed MnO_2 dissolution on reduction in excess free electrolyte and this can lead to mechanical disintegration during cycling [33].

The best rechargeability is achieved when the CM material [3, 22] is diluted with a large proportion of high-area graphite and/or when the electrode is cycled in a 'starved electrolyte' cell, i.e., one containing the absolute minimum of free electrolyte/solution. Then maximization of rechargeability is attained because the soluble manganese intermediate remains in contact with the graphite so that the required further reactions can occur or, on account of the small free electrolyte volume, the intermediate(s) saturate(s) the electrolyte and/or are adsorbed on the solid particles and cannot further diffuse away from the electrode.

In another series of experiments, bismuth species (as Bi_2O_3) were introduced directly into the electrolyte while the MnO_2 electrode was subjected to cyclic voltammetry; the rechargeability was improved somewhat, although the effects were not as dramatic as for deposits of MnO_2 with directly included bismuth species.

3.4. *Effects of porosity or roughness, and graphite content*

To investigate the effect of the porosity and roughness of graphite on the cycling behaviour of deposited

Table 3. Anodic recharge behaviour achieved after various extents of cycling with and without bismuth present

Cycle	*Charge with bismuth*/mC cm^{-2}	*Charge without bismuth*/mC cm^{-2}
	Anodic	Anodic
1	37	39
5	35	30
30		12
40	41	
640	40	

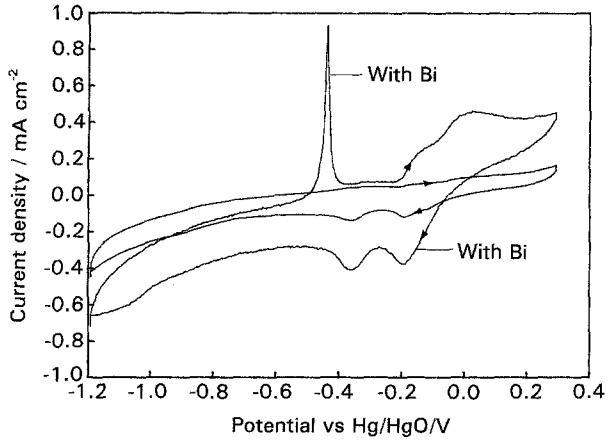

Fig. 7. Cyclic voltammetry of MnO_2 deposits on glassy carbon with and without bismuth species in the deposit. Electrolyte 9 M aq. KOH, 298 K.

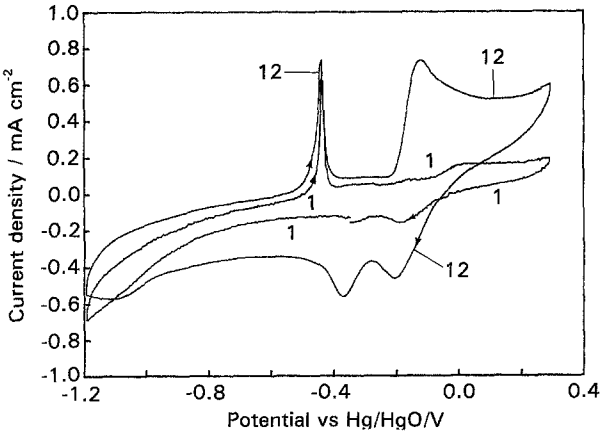

Fig. 8. Cyclic voltammetry of an MnO_2 deposit with bismuth species on glassy carbon. The 1st and 12th cycles are shown. Electrolyte 9 M aq. KOH, 298 K.

MnO_2, several comparative experiments were conducted on glassy carbon. This material is effectively nonporous and relatively smooth in comparison with regular graphite. For these experiments, MnO_2 was deposited only on the end of a 7 mm diameter rod (i.e., area 0.384 cm^2) and then cycled in the 'rod end' cell (Fig. 2). Deposits on the glassy carbon generally had good appearance but were not well adherent. Cyclic voltammetry was conducted at a sweep-rate of 5 mV s^{-1}.

Figure 7 shows a comparison between the current responses on the third cycles at deposits made with and without bismuth. The deposition baths contained 0.5 M Mn and 0.5 M H_2SO_4 and the bath for codeposition of bismuth was 0.005 M in Bi. The principal feature of Fig. 7 is that the cycling capacity is again much larger with bismuth in the deposit. Figure 8 shows that the capacity of the deposit with bismuth increases with cycling, the 1st and 12th cycles being shown. After the 12th cycle, however, the capacity declined slowly. The charge associated with the anodic manganese peak is 0.066 C cm^{-2}. This is still relatively small when compared with the 0.6 C cm^{-2} used to make the deposit. This shows how important is the available contact area of the carbon in facilitating the cycling behaviour.

To illustrate this point further, the experiment was repeated but with about 10 mg of Lonza graphite in the form of a paste with 9 M KOH being added to the cell. This material was sandwiched between the end of the electrode and the Celgard separator, providing an intimate contact between the graphite and the deposit. Figure 9 shows a comparison between cycling of MnO_2 deposits (with included bismuth species) with and without the graphite. Note that these voltammograms are plotted on a five-times larger current scale than in the previous two figures. The charge capacity of the deposit cycled with graphite quickly increases with cycling so that the capacity by the third cycle, as shown, is markedly higher than that after cycling without graphite. The charge of the anodic manganese peak with graphite is 0.27 C cm^{-2}, a value which is now much closer to the charge used to generate the deposit. This experiment highlights the fact that a large surface area of graphite is required but it also provides support for the soluble intermediate pathway [9, 22] for the charge–discharge mechanism, as the manganese must become soluble at some point in order to become transferred to the graphite and exhibit electroactivity, presumably at its surface. Excess graphite also improves contact of the active matrix with the current collector.

The voltammograms presented in this section are more complicated than those shown earlier. The extended sweep range reveals some features not previously resolved; for example, there is a significant cathodic peak at about −0.8 V which is always accompanied by an anodic tail extending to ca. 0.2 V. These features are conjugate to each other as shown by successive limitations of the sweep range of the voltammogram. The tentative assignment of these peaks is that they arise from redox reactions of a loosely bound overlayer of $Mn(OH)_2/MnO_2$; they are only observed when bismuth species are present, implying that the bismuth species may improve the conductivity of the underlying deposit or catalyze nucleation of the Mn-species involved. Although the

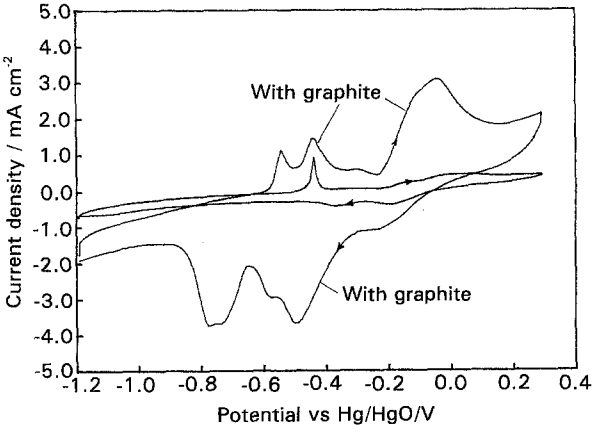

Fig. 9. Cyclic voltammetry of MnO_2 deposits, with included bismuth species, with and without Lonza graphite added to the working electrode compartment. The 3rd cycle for each is shown. Electrolyte 9 M aq. KOH, 298 K.

charge associated with these peaks can become substantial, it is of little practical use for a battery system due to the potential at which the reduction occurs and the large overpotential required to reoxidize the reduced product. The occurrence of these peaks is not limited to deposits of MnO_2 on glassy carbon; they are also observed when deposits on porous graphite are cycled and when Mn metal itself is cycled in a 9 M KOH electrolyte containing bismuth species. However, these peaks were small or nonexistent when regular chemically modified MnO_2 was subjected to cyclic voltammetry in other work in our laboratory [22].

The other peaks shown in Fig. 9 are associated with the normal reduction and reoxidation processes at MnO_2 except for the anodic peaks arising around -0.55 to -0.45 V which are associated with the oxidation of Bi^0 to Bi^{3+} while the corresponding reduction peaks arise between -0.65 and -0.70 V but they are not resolved when the large manganese-process current peaks arise over that potential range.

4. Conclusions

The following conclusions may be drawn.

(i) Good deposits of MnO_2 with included bismuth species can be produced by anodic deposition from sulphuric acid.

(ii) The results suggest that the bismuth is included in the MnO_2 deposit by the precipitation of $Bi_2(SO_4)_3$ or $BiH(SO_4)_2$ caused by local acidity produced by the MnO_2 deposition reaction.

(iii) Deposits formed in this way show much enhanced rechargeability when compared with that for MnO_2 deposited without bismuth species.

(iv) Although the role of bismuth in the enhancement of rechargeability is not fully understood, it may act in some way to enhance the nucleation and growth of solid species from the soluble intermediates that have been detected and/or provide a pathway which avoids irreversible formation of Mn_3O_4 [33].

(v) For possible use of this cathode in a small practical battery, the volume of free electrolyte would have to be kept to a minimum, maintaining a 'starved-electrolyte' condition.

Acknowledgements

Grateful acknowledgment is made to the Natural Sciences and Engineering Research Council of Canada for support of this work through a Strategic Grant. We also thank Dr H. S. Wroblowa for useful discussions, as a consultant on this project and Dr W. A. Adams of ESTCO, University of Ottawa, for his interest and practical involvement in this work.

References

[1] Y. F. Yao, N. Gupta, H. S. Wroblowa, *J. Electroanal. Chem.* **223** (1987) 107.
[2] H. S. Wroblowa and N. Gupta, *ibid.* **238** (1987) 98.
[3] M. A. Dzieciuch, N. Gupta and H. S. Wroblowa, *J. Electrochem. Soc.* **135** (1988) 2415.
[4] H. S. Wroblowa, N. Gupta and Y. F. Yao, *Battery Materials Symposium*, Graz **2** (1985) 203.
[5] M. A. Dzieciuch, H. S. Wroblowa and J. T. Kummer, *US Patent 4 451 543* (1984).
[6] Y. Y. Yao, *US Patent 4 520 005* (1985).
[7] K. Kordesch, J. Gsellmann, M. Peri, K. Tomantschger and R. Chemelli, *Electrochim. Acta* **26** (1981) 1495.
[8] A. Kozawa and J. F. Yeager, *J. Electrochem. Soc.* **112** (1965) 959.
[9] A. Kozawa and R. A. Powers, *ibid.* **113** (1966), 870.
[10] *Idem, Electrochem. Tech.* **5** (1967) 535.
[11] *Idem, ibid.* **115** (1968) 122.
[12] *Idem, ibid.* **115** (1968) 1003.
[13] *Idem, J. Chem. Educ.* **49** (1972) 587.
[14] N. C. Cahoon and M. P. Korver, *J. Electrochem. Soc.* **100** (1959) 745.
[15] G. S. Bell and R. Huber, *ibid.* **111** (1964) 1.
[16] P. Ruetschi, *ibid.* **123** (1976) 495.
[17] A. Era, Z. Takehara and S. Yoshizawa, *Electrochim. Acta* **13** (1968) 207.
[18] W. C. Vosburgh and Pao-soong Lou, *J. Electrochem. Soc.* **108** (1961) 485.
[19] D. Boden, C. J. Venuto, D. Wisler and R. B. Wylie, *ibid.* **114** (1967) 415.
[20] K. J. Vetter, *Z. Elektrochem.* **66** (1962) 577.
[21] K. J. Vetter, *J. Electrochem. Soc.* **110** (1963) 597.
[22] D. Y. Qu, B. E. Conway, L. Bai, Y. H. Zhou and W. A. Adams, *ibid.* **140** (1993) 884; see also. *J. Electroanal. Chem.* **365** (1994) 247.
[23] G. D. van Arsdale and C. G. Maier, *Trans. Electrochem. Soc.* **33** (1918) 109.
[24] G. W. Nichols, *ibid.* **62** (1932) 393.
[25] O. W. Storey, E. Steinhoff and E. R. Hoff, *ibid.* **86** (1944) 337.
[26] F. B. Allan, *Am. Chem. J.* **27** (1902) 284.
[27] S. Skramovsky and O. Vondrasek, *Coll. Czech. Chem. Commun.* **9** (1937) 329.
[28] A. Kozawa, T. Kalnok-kis and J. F. Yeager, *J. Electrochem. Soc.* **113** (1966) 405.
[29] K. A. K. Lott and M. C. R. Symons, *J. Chem. Soc., Lond.* (1959) 829.
[30] E. Preisler, *Battery Material Symposium*, Graz **2** (1985) 247.
[31] L. Bai, L. Gao and B. E. Conway, *J. Chem. Soc., Faraday Trans.* **89** (1993) 235.
[32] L. Bai, L. Gao and B. E. Conway, [31], part 2 *J. Chem. Soc., Faraday Trans.* **89** (1993) 243.
[33] J. McBreen, *Power Sources* **5** (1975) 525.
[34] A. J. Bard, R. Parsons and J. Jordan (Eds), Standard potentials in aqueous solution, Marcel Dekker, New York (1985), IUPAC publication.